

# Synthetic Transformation of 2-{2-Fluoro[1,1'-biphenyl]-4-yl} Propanoic Acid into Hydrazone–Hydrazone Derivatives: *In Vitro* Urease Inhibition and *In Silico* Study

Sajjad Ahmad, Momin Khan,\* Muhammad Ishaq Ali Shah, Mahboob Ali, Aftab Alam, Muhammad Riaz, and Khalid Mohammed Khan



Cite This: *ACS Omega* 2022, 7, 45077–45087



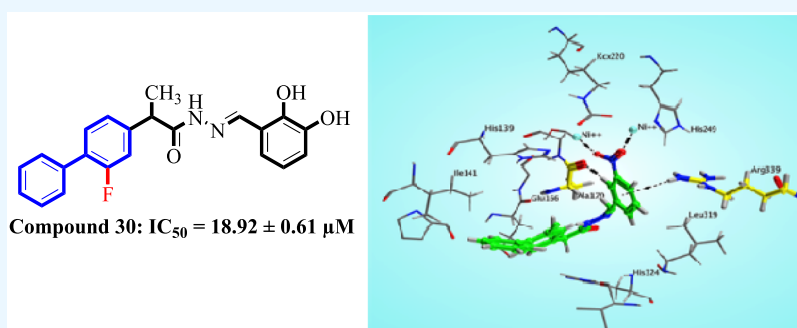
Read Online

ACCESS |

Metrics & More

Article Recommendations

Supporting Information



Compound 30:  $IC_{50} = 18.92 \pm 0.61 \mu M$

**ABSTRACT:** In the present study, 28 acyl hydrazones (4–31) of flurbiprofen were synthesized in good to excellent yield by reacting different aromatic aldehydes with the commercially available drug flurbiprofen. The compounds were deduced with the help of different spectroscopic techniques like  $^1H$ -NMR and HREI-MS and finally evaluated for *in vitro* urease inhibitory activity. All of the synthesized products demonstrated good inhibitory activities in the range of  $IC_{50} = 18.92 \pm 0.61$  to  $90.75 \pm 7.71 \mu M$  as compared to standard thiourea ( $IC_{50} = 21.14 \pm 0.42 \mu M$ ). Compound 30 was found to be the most active among the series better than the standard thiourea. A structure–activity relationship (SAR) study revealed that the presence of electron-donating groups on the phenyl ring plays a prominent role in the inhibition of the urease enzyme. Moreover, *in silico* molecular modeling analysis was carried out to study the effect of substituents in synthesized derivatives on the binding interactions with the urease enzyme.

## INTRODUCTION

Urease belongs to the family of amid hydrolases with two nickel atoms in their core structure. This enzyme catalyzes the hydrolysis of urea into carbon dioxide and ammonia. The high activity of urease releases too much ammonia, causing the stomach to become alkaline,<sup>1</sup> which favors the survival of *Helicobacter pylori* (HP), which leads to the development of gastric and peptic ulcers, which can eventually lead to cancer.<sup>2</sup> Nitrogen metabolism in cattle and various other animals is controlled by the action of urease.<sup>3</sup> A prominent increase in the level of these enzymes can lead to a variety of diseases, as it helps in the survival of some bacterial pathogens.<sup>4</sup> Elevated ammonia levels also cause several metabolic disturbances and damage GIT epithelial cells. Many compounds belonging to different classes have been reported as urease inhibitors, such as hydroxamic derivatives, phosphodiamidates, thiolates bound to the nickel atom of the enzyme, and a few peptide chains having a ligand that may chelate with nickel of urease. Unfortunately, these molecules have undesirable side effects; therefore, it is crucial to find more urease inhibitors with low toxicity, remarkable stability, and bioavailability.<sup>5</sup>

Day by day, the chemistry of hydrazone is fastly becoming the backbone for the condensation reaction in benzo-fused *N*-heterocycles. Hydrazides are an important class of functional groups in organic chemistry possessing the  $-NH-N=CH-$  groups with the availability of proton that aids their pharmaceutical importance. The remedial possibilities of acid hydrazides gained momentum after the innovation of isonicotinic acid hydrazone (INH). The remarkable clinical value of INH<sup>6,7</sup> stimulated the study of other heterocyclic hydrazides possessing monocyclic nuclei like furan, pyrrole, thiophene, and dicyclic nuclei like quinoline and isoquinoline. Benzohydrazides are reported to possess a wide variety of biological activities like antiglycation,<sup>8–11</sup> antioxidation,<sup>12–14</sup>

Received: August 26, 2022

Accepted: November 8, 2022

Published: November 30, 2022



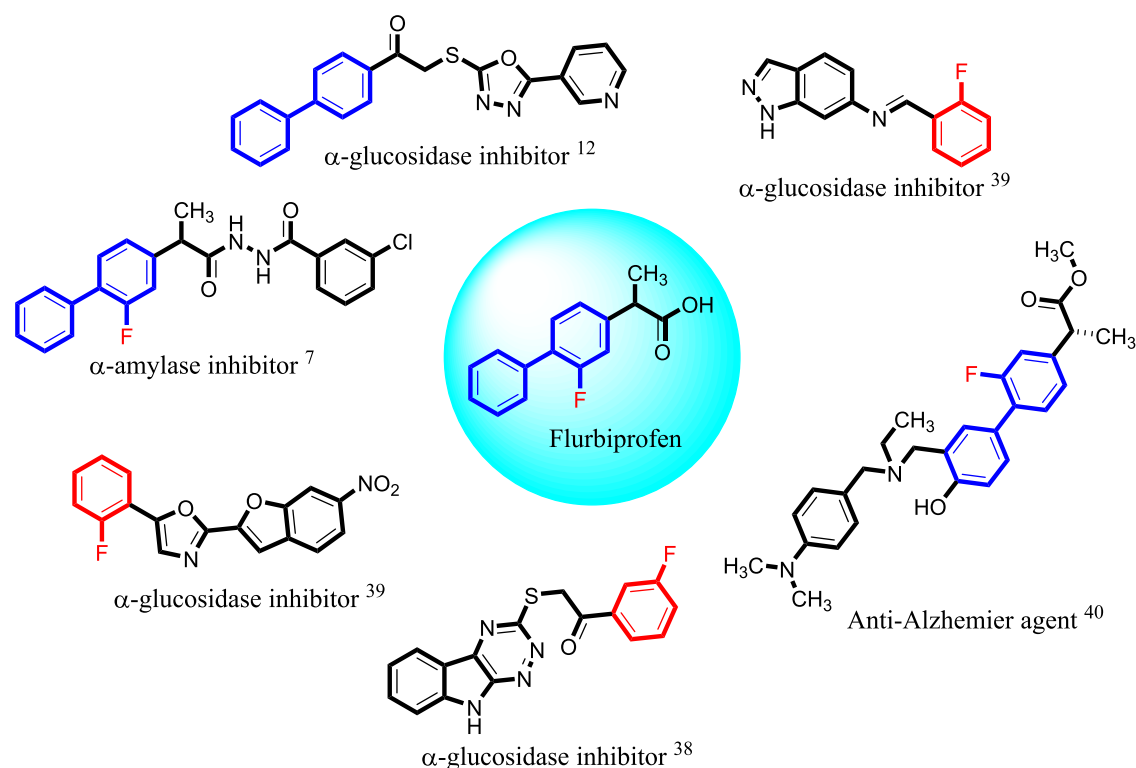


Figure 1. Justification of the current study.

antileishmanial,<sup>15</sup> antibacterial,<sup>16</sup> antifungal,<sup>17</sup> antitumor,<sup>18</sup> and anticonvulsion.<sup>19–22</sup>

The nonsteroidal anti-inflammatory drugs (NSAIDs) having free carboxylic acid group are a diverse class of medicines with similar biocompetencies that are used throughout the world.<sup>23</sup> These are a class of medications with analgesic, anti-inflammatory, or antipyretic characteristics that are used to reduce or eliminate pain, erythema, inflammation, and fever.<sup>24</sup> They can be used clinically to relieve pain in a variety of conditions, like postoperative pain, menstrual cramps, and arthritic pain.<sup>25,26</sup> The nonsteroidal anti-inflammatory drugs are well-known anti-inflammatory medications because they work by preventing the production of prostaglandins by decreasing the activity of cyclooxygenase enzymes (COX-I and COX-II).<sup>27</sup> The use of NSAIDs to treat and prevent cancer has been the subject of more investigation in recent years, but the link between chronic inflammation and cancer has long been known.<sup>28</sup>

Flurbiprofen, also known as 2-(4-phenyl-3-fluorophenyl)propanoic acid, is a member of the nonsteroidal anti-inflammatory drugs that is present as a chiral compound with stereoselective nature in humans.<sup>29</sup> Since its introduction to the market in Europe in 1977, it has been widely used to treat arthritis.<sup>30</sup> Moreover, it is used for the treatment of migraine,<sup>31</sup> acute gout,<sup>32</sup> osteoarthritis,<sup>33</sup> soft tissue injuries, bursitis, and tendinitis,<sup>34</sup> rheumatoid arthritis,<sup>35</sup> postoperative ocular inflammation,<sup>36</sup> and excimer laser photorefractive keratectomy.<sup>37</sup>

In this study, we proposed to synthesize a number of analogues from a commercially available drug flurbiprofen through the installation of a biologically active pharmacophore and to screen the compounds for various biological potentials. It is important to note that the newly prepared derivatives contain structural moieties like hydrazide and different

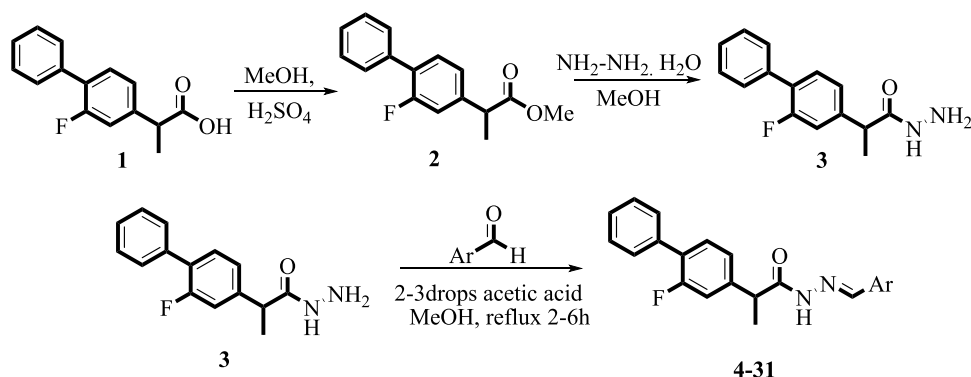
substituted aldehyde functionalities, which are the fundamental components of the enzyme inhibitors that have already been identified. Khan et al. reported various substituted oxadiazole derivatives of flurbiprofen and evaluated their *in vitro*  $\alpha$ -amylase inhibitory activity, which showed excellent results.<sup>7</sup> Moreover, compounds containing biphenyl rings were screened for  $\alpha$ -glucosidase inhibitory potential as well as anti-Alzheimer activity and considered as lead molecules for type II diabetes mellitus (DM) (Figure 1).<sup>38–40</sup> Similarly, Bushra et al. have reported the potent  $\alpha$ -glucosidase inhibitory activity of different compounds containing fluorine atoms attached to the benzene rings and confirmed that the fluorine atoms are responsible for the potential of the compounds.<sup>39</sup> This motivated us to screen these derivatives (4–31) for *in vitro* urease inhibitory potential.

## EXPERIMENTAL SECTION

**Materials and Methods.** NMR spectra were performed on Avance-Bruker (400 MHz for <sup>1</sup>H). VG Analytical ZAB-E instrument (EPSRC Mass Spectrometry Service, Swansea) was used to record the high- and low-resolution mass spectra of compounds. Aluminum plates, coated with Merck Kieselgel 60 GF254, were used for TLC analysis. UV light of 254 nm and/or 366 nm was used to visualize and confirm the formation of products. In some cases, the sulfuric acid reagent was also applied as a spraying agent to locate the spot on a chromatogram plate.

Solvents used in this work were analytical grade and purchased from Merck (Germany). Various substituted aromatic benzaldehydes and 2-(2-fluoro-[1,1'-biphenyl]-4-yl)propanoic acid (CAS No. 5104-49-4) were purchased from Sigma Aldrich (St Louis, MO). Sodium hydroxide, soluble starch, maltose, and other chemicals were obtained from Merck (Darmstadt, Germany).

**Scheme 1. General Scheme for the Synthesis of (*E*)-*N'*-Benzylidene-2-(2-fluoro-[1,1'-biphenyl]-4-yl)propanehydrazide Derivatives (4–31)**



**General Procedure for the Synthesis of Flurbiprofen Ester (2).** The commercially available drug flurbiprofen **1** was refluxed with sulfuric acid ( $\text{H}_2\text{SO}_4$ ) in methanol solvent to obtain the desired flurbiprofen ester **2**. In a typical reaction, 2 g of flurbiprofen acid was dissolved in a 100 mL round-bottom flask (RB flask) and sulfuric acid was added to the flask. The reaction mixture was refluxed for 5–6 h. The progress of the reaction was monitored using thin-layer chromatography with a solvent system of *n*-hexane and ethyl acetate (2:8). After the completion, it was poured onto a beaker containing crushed ice. Then, the reaction was neutralized with sodium bicarbonate solution and extracted with chloroform ( $3 \times 30 \text{ mL}^2$ ) to obtain the desired esters of flurbiprofen. The organic layer containing ester was dried under the air and collected for further reactions. This compound was reported by Khan et al.<sup>7</sup>

**General Procedure for the Synthesis of Flurbiprofen Hydrazone and Hydrazones (3–31).** The synthesized ester **2** was taken in a 100 mL RB flask containing 20 mL of methanol. Then, 2.5 mL of hydrazine hydrate was added and the reaction was refluxed for 3–4 h. The forward direction of the reaction was checked by TLC with a 40% polar solvent system of ethyl acetate and *n*-hexane. After the completion of the reaction, the mixture was poured into a beaker containing ice-cold distilled water. The precipitates were formed, filtered, washed with excess water, and dried under the air. The desired precipitates were further reacted with different aromatic substituted aldehydes in the presence of acetic acid to get the desired hydrazones (**4–31**) of flurbiprofen hydrazide. The compounds were purified through recrystallization and characterized with the help of HREI-MS and  $^1\text{H-NMR}$  spectroscopy (Scheme 1).

**Urease Inhibition Assay.** Urease inhibitory activity was performed according to the reported method.<sup>40–42</sup> Briefly, 40  $\mu\text{L}$  of phosphate buffers at pH 6.8, 10  $\mu\text{L}$  of the synthesized derivatives, and 10  $\mu\text{L}$  of the enzyme were incubated for 10 min at 37  $^\circ\text{C}$  in a 96-well plate. To each well, 40  $\mu\text{L}$  of solutions of the phenol reagent and 40  $\mu\text{L}$  of alkali reagent were added. The experiment was performed in a triplicate manner. The absorbance was read at 625 nm using a Microplate reader (Bio-TekELx 800, Instruments, Inc.). In this case, the standard inhibitor was thiourea. The percentage inhibition was calculated using the equation

$$\% \text{ inhibition} = \frac{(\text{absorbance control} - \text{absorbance sample})}{\text{absorbance control}} \times 100$$

**Docking Methodology.** For predicting the mechanism of inhibition and binding mode of the synthesized compounds,

molecular docking of the active compounds was performed with the active sites in the crystalline structure of the urease enzyme using a molecular operating environment.<sup>43,44</sup> The builder tool implemented in molecular operating environment software was used to build the three-dimensional structures of isolated compounds. After using the default parameters of the MOE (Force Field: MMFF94X gradient: 0.05), it was observed that the active compounds were energy minimized and 3D protonated. A protein data bank (PDB ID 4ubp) was used to retrieve the 3-D structure of the target protein, Jack Bean Urease. The 3D protonation was carried out after the removal of water molecules. Parameters of MOE used for docking studies were Placement: Triangle Matcher, Rescoring 1: London dG, Refinement: Force field, Rescoring 2: GBVI/WSA. Formation of 10 conformations was allowed for each ligand and conformations of maximum docking score were top in ranking and selected for further analysis.

**Analysis of Physical and Spectroscopic Data of Hydrazones.** 2-(2-Fluoro-[1,1'-biphenyl]-4-yl)-*N'*-(naphthalen-1-ylmethylene)propanehydrazide (**4**). Color: white; *Rf*: 0.51 (*n*-hexane/ethyl acetate 25:75);  $^1\text{H-NMR}$  (400 MHz  $\text{DMSO-}d_6$ )  $\delta$  1.69 (d,  $J = 6.8 \text{ Hz}$ , 3H), 3.82 (d,  $J = 7.0 \text{ Hz}$ , 1H), 7.10 (m, 1H), 7.34–7.50 (m, 5H), 7.59–7.61 (m, 4H), 7.77 (d,  $J = 8.0 \text{ Hz}$ , 2H), 7.83 (d,  $J = 7.8 \text{ Hz}$ , 2H), 7.95 (t,  $J = 7.8 \text{ Hz}$ , 1H), 8.46 (s, 1H), 11.6 (s, 1H); HRESI-MS [ $\text{M} + \text{H}$ ]<sup>+</sup> calcd for  $\text{C}_{26}\text{H}_{21}\text{FN}_2\text{O}$ , 396.16, found, 396.4561.

2-(2-Fluoro-[1,1'-biphenyl]-4-yl)-*N'*-(2,3,4-trihydroxybenzylidene)propanehydrazide (**5**). Color: Cream; *Rf*: 0.53 (*n*-hexane/ethyl acetate 25:75);  $^1\text{H-NMR}$  (400 MHz  $\text{DMSO-}d_6$ )  $\delta$  1.54 (d,  $J = 6.7 \text{ Hz}$ , 3H), 3.89 (d,  $J = 7.0 \text{ Hz}$ , 1H), 7.10–7.15 (m, 5H), 7.75 (d,  $J = 7.8 \text{ Hz}$ , 2H), 7.83–7.86 (m, 3H), 8.49 (s, 1H), 9.87 (s, 1H), 10.2 (s, 2H), 11.59 (s, 1H); HRESI-MS [ $\text{M} + \text{H}$ ]<sup>+</sup> calcd for  $\text{C}_{22}\text{H}_{19}\text{FN}_2\text{O}_4$ , 394.1329, found, 394.3957.

*N'*-(2-Aminobenzylidene)-2-(2-fluoro-[1,1'-biphenyl]-4-yl)propanehydrazide (**6**). Color: Creamy *Rf*: 0.48 (*n*-hexane/ethyl acetate 25:75);  $^1\text{H-NMR}$  (400 MHz  $\text{DMSO-}d_6$ )  $\delta$  1.32 (d,  $J = 7.0 \text{ Hz}$ , 3H), 3.37 (s, 2H), 3.60 (q,  $J = 7.2 \text{ Hz}$ , 1H), 7.41–7.53 (m, 4H), 7.81 (d,  $J = 7.8 \text{ Hz}$ , 2H), 7.85 (t,  $J = 8.2 \text{ Hz}$ , 2H), 7.94–8.12 (m, 4H), 8.51 (s, 1H), 11.44 (s, 1H); HRESI-MS [ $\text{M} + \text{H}$ ]<sup>+</sup> calcd for  $\text{C}_{22}\text{H}_{20}\text{FN}_3\text{O}$ , 361.1590, found, 361.4121.

2-(2-Fluoro-[1,1'-biphenyl]-4-yl)-*N'*-(3-nitrobenzylidene)propanehydrazide (**7**). Color: White; *Rf*: 0.52 (*n*-hexane/ethyl acetate 25:75);  $^1\text{H-NMR}$  (400 MHz  $\text{DMSO-}d_6$ )  $\delta$  1.41 (d,  $J = 7.2 \text{ Hz}$ , 3H), 3.60 (q,  $J = 7.2 \text{ Hz}$ , 1H), 7.31–7.33 (m, 5H),

7.56 (d,  $J = 7.0$  Hz, 1H), 7.81 (d,  $J = 7.0$  Hz, 1H), 7.87–7.90 (m, 2H), 8.12 (d,  $J = 8.5$  Hz, 1H), 8.34 (t,  $J = 8.5$  Hz, 1H), 8.53 (s, 1H), 8.61 (d,  $J = 8.5$  Hz, 1H), 11.23 (s, 1H); HRESI-MS  $[M + H]^+$  calcd for  $C_{22}H_{18}FN_3O_3$ , 391.1332, found, 391.3950.

*N'*-(5-Bromo-2-methoxybenzylidene)-2-(2-fluoro-[1,1'-biphenyl]-4-yl)propanehydrazide (**8**). Color: White; Rf: 0.54 (*n*-hexane/ethyl acetate 25:75);  $^1H$ -NMR (400 MHz DMSO- $d_6$ )  $\delta$  1.45 (d,  $J = 7.0$  Hz, 3H), 3.49 (q,  $J = 7.0$  Hz, 1H), 3.65 (s, 3H), 7.28–7.30 (m, 5H), 7.42 (d,  $J = 7.5$  Hz, 1H), 7.67 (d,  $J = 7.5$  Hz, 1H), 7.71–7.73 (m, 3H), 7.86 (d,  $J = 7.5$  Hz, 1H), 8.49 (s, 1H), 11.61 (s, 1H); HRESI-MS  $[M + H]^+$  calcd for  $C_{23}H_{20}BrFN_2O_2$ , 454.0692, found, 455.3195.

2-(2-Fluoro-[1,1'-biphenyl]-4-yl)-*N'*-(2,3,4-trimethoxybenzylidene)propanehydrazide (**9**). Color: Brown; Rf: 0.51 (*n*-hexane/ethyl acetate 25:75);  $^1H$ -NMR (400 MHz DMSO- $d_6$ )  $\delta$  1.45 (d,  $J = 7.0$  Hz, 3H), 3.49 (q,  $J = 7.0$  Hz, 1H), 3.65 (s, 6H), 3.66 (s, 3H), 7.31–7.33 (m, 4H), 7.29 (d,  $J = 7.0$  Hz, 1H), 7.36 (d,  $J = 7.0$  Hz, 2H), 7.48–7.50 (m, 3H), 8.45 (s, 1H), 11.57 (s, 1H); HRESI-MS  $[M + H]^+$  calcd for  $C_{25}H_{25}FN_2O_4$ , 436.1798, found, 436.4754.

*N'*-(2-Chloro-5-nitrobenzylidene)-2-(2-fluoro-[1,1'-biphenyl]-4-yl)propanehydrazide (**10**). Color: Cream; Rf: 0.49 (*n*-hexane/ethyl acetate 25:75);  $^1H$ -NMR (400 MHz DMSO- $d_6$ )  $\delta$  1.36 (d,  $J = 7.3$  Hz, 3H), 3.48 (q,  $J = 7.3$  Hz, 1H), 7.18–7.21 (m, 4H), 7.52 (d,  $J = 7.6$  Hz, 1H), 7.68 (d,  $J = 7.6$  Hz, 1H), 7.82–7.84 (m, 3H), 8.47 (d,  $J = 8.4$  Hz, 1H), 8.49 (d,  $J = 1.5$  Hz, 1H), 8.55 (s, 1H), 11.51 (s, 1H); HRESI-MS  $[M + H]^+$  calcd for  $C_{22}H_{17}ClFN_3O_3$ , 425.0942, found, 425.8401.

*N'*-(4-Ethoxy-2-methoxybenzylidene)-2-(2-fluoro-[1,1'-biphenyl]-4-yl)propanehydrazide (**11**). Color: Cream; Rf: 0.52 (*n*-hexane/ethyl acetate 25:75);  $^1H$ -NMR (400 MHz DMSO- $d_6$ )  $\delta$  1.41 (d,  $J = 6.8$  Hz, 3H), 1.81 (t,  $J = 6.8$  Hz, 3H), 3.49 (q,  $J = 6.8$  Hz, 1H), 3.63 (q,  $J = 6.6$  Hz, 2H), 3.65 (s, 3H), 7.11–7.12 (m, 5H), 7.23 (d,  $J = 7.2$  Hz, 1H), 7.32 (d,  $J = 7.2$  Hz, 2H), 7.51 (m, 3H), 8.42 (s, 1H), 11.52 (s, 1H); HRESI-MS  $[M + H]^+$  calcd for  $C_{25}H_{25}FN_2O_3$ , 420.1849, found, 420.4760.

*N'*-(4-Fluoro-3-methoxybenzylidene)-2-(2-fluoro-[1,1'-biphenyl]-4-yl)propanehydrazide (**12**). Color: Cream; Rf: 0.52 (*n*-hexane/ethyl acetate 25:75);  $^1H$ -NMR (400 MHz DMSO- $d_6$ )  $\delta$  1.43 (d,  $J = 7.1$  Hz, 3H), 3.44 (q,  $J = 7.1$  Hz, 1H), 3.62 (s, 3H), 7.34–7.36 (m, 5H), 7.59 (d,  $J = 7.4$  Hz, 1H), 7.71–7.77 (m, 5H), 8.48 (s, 1H), 11.49 (s, 1H); HRESI-MS  $[M + H]^+$  calcd for  $C_{23}H_{20}F_2N_2O_2$ , 394.1493, found, 394.4139.

*N'*-(3-Ethoxy-4-methoxybenzylidene)-2-(2-fluoro-[1,1'-biphenyl]-4-yl)propanehydrazide (**13**). Color: Cream; Rf: 0.53 (*n*-hexane/ethyl acetate 25:75);  $^1H$ -NMR (400 MHz DMSO- $d_6$ )  $\delta$  1.44 (d,  $J = 7.1$  Hz, 3H), 1.80 (t,  $J = 6.9$  Hz, 3H), 3.45 (q,  $J = 6.9$  Hz, 1H), 3.62 (q,  $J = 7.1$  Hz, 2H), 3.67 (s, 3H), 7.14–7.16 (m, 5H), 7.27 (d,  $J = 7.3$  Hz, 1H), 7.31 (d,  $J = 7.3$  Hz, 2H), 7.51–7.53 (m, 3H), 8.47 (s, 1H), 11.39 (s, 1H); HRESI-MS  $[M + H]^+$  calcd for  $C_{25}H_{25}FN_2O_3$ , 420.1849, found, 420.4760.

*N'*-(2,6-Dimethoxybenzylidene)-2-(2-fluoro-[1,1'-biphenyl]-4-yl)propanehydrazide (**14**). Color: Cream; Rf: 0.52 (*n*-hexane/ethyl acetate 25:75);  $^1H$ -NMR (400 MHz DMSO- $d_6$ )  $\delta$  1.41 (d,  $J = 7.0$  Hz, 3H), 3.42 (q,  $J = 7.0$  Hz, 1H), 3.69 (s, 6H), 7.11–7.14 (m, 5H), 7.29 (t,  $J = 7.0$  Hz, 1H), 7.33 (d,  $J = 7.0$  Hz, 2H), 7.52–7.54 (m, 3H), 8.43 (s, 1H), 11.60 (s, 1H); HRESI-MS  $[M + H]^+$  calcd for  $C_{24}H_{23}FN_2O_3$ , 406.1693, found, 406.4494.

(*E*)-2-(2-Fluoro-[1,1'-biphenyl]-4-yl)-*N'*-(4-nitrobenzylidene)propanehydrazide (**15**). Color: Cream; Rf:

0.52 (*n*-hexane/ethyl acetate 25:75);  $^1H$ -NMR (400 MHz DMSO- $d_6$ )  $\delta$  1.42 (d,  $J = 6.7$  Hz, 3H), 3.42 (q,  $J = 6.7$  Hz, 1H), 7.11–7.14 (m, 5H), 7.52–7.54 (m, 3H), 7.73 (d,  $J = 8.5$  Hz, 2H), 8.43 (s, 1H), 8.67 (d,  $J = 8.5$  Hz, 2H), 11.49 (s, 1H); HRESI-MS  $[M + H]^+$  calcd for  $C_{22}H_{18}FN_3O_3$ , 391.1332, found, 391.3950.

(*E*)-*N'*-(2-Chloro-3,4-dimethoxybenzylidene)-2-(2-fluoro-[1,1'-biphenyl]-4-yl)propanehydrazide (**16**). Color: Light brown; Rf: 0.53 (*n*-hexane/ethyl acetate 25:75);  $^1H$ -NMR (400 MHz DMSO- $d_6$ )  $\delta$  1.39 (d,  $J = 6.9$  Hz, 3H), 3.38 (q,  $J = 6.9$  Hz, 1H), 3.82 (s, 3H), 3.84 (s, 3H), 7.32–7.34 (m, 5H), 7.46 (d,  $J = 7.3$  Hz, 1H), 7.49 (d,  $J = 7.2$  Hz, 2H), 7.55–7.58 (m, 3H), 8.60 (s, 1H), 11.59 (s, 1H); HRESI-MS  $[M + H]^+$  calcd for  $C_{24}H_{22}ClFN_2O_3$ , 440.1303, found, 440.8945.

2-(2-Fluoro-[1,1'-biphenyl]-4-yl)-*N'*-(3-nitrobenzylidene)propanehydrazide (**17**). Color: White; Rf: 0.51 (*n*-hexane/ethyl acetate 25:75);  $^1H$ -NMR (400 MHz DMSO- $d_6$ )  $\delta$  1.43 (d,  $J = 7.1$  Hz, 3H), 3.45 (q,  $J = 7.1$  Hz, 1H), 7.35–7.39 (m, 7H), 7.48 (d,  $J = 7.0$  Hz, 1H), 7.48 (d,  $J = 7.6$  Hz, 2H), 7.53 (d,  $J = 7.6$  Hz, 2H), 7.51–7.56 (m, 5H), 8.51 (s, 1H), 11.47 (s, 1H); HRESI-MS  $[M + H]^+$  calcd for  $C_{28}H_{23}FN_2O_2$ , 438.1744, found, 438.4928.

2-(2-Fluoro-[1,1'-biphenyl]-4-yl)-*N'*-(3-methoxy-4-phenoxybenzylidene)propanehydrazide (**18**). Color: White; Rf: 0.49 (*n*-hexane/ethyl acetate 25:75);  $^1H$ -NMR (400 MHz DMSO- $d_6$ )  $\delta$  1.47 (d,  $J = 7.0$  Hz, 3H), 3.49 (q,  $J = 7.0$  Hz, 1H), 3.92 (s, 3H), 7.14–7.18 (m, 6H), 7.48 (s, 1H), 7.48 (d,  $J = 7.6$  Hz, 1H), 7.57–7.60 (m, 6H), 7.87 (t,  $J = 7.0$  Hz, 2H), 8.63 (s, 1H), 11.63 (s, 1H); HRESI-MS  $[M + H]^+$  calcd for  $C_{29}H_{25}FN_2O_3$ , 468.1849, found, 468.5188.

2-(2-Fluoro-[1,1'-biphenyl]-4-yl)-*N'*-(2-methoxybenzylidene)propanehydrazide (**19**). Color: White; Rf: 0.52 (*n*-hexane/ethyl acetate 25:75);  $^1H$ -NMR (400 MHz DMSO- $d_6$ )  $\delta$  1.35 (d,  $J = 7.0$  Hz, 3H), 3.45 (q,  $J = 7.0$  Hz, 1H), 3.94 (s, 3H), 7.17–7.19 (m, 4H), 7.27 (d,  $J = 7.6$  Hz, 1H), 7.34 (t,  $J = 7.6$  Hz, 2H), 7.47 (d,  $J = 7.6$  Hz, 1H), 7.58–7.60 (m, 4H), 8.46 (s, 1H), 11.48 (s, 1H); HRESI-MS  $[M + H]^+$  calcd for  $C_{23}H_{21}FN_2O_2$ , 376.1587, found, 376.4234.

*N'*-(4-Bromobenzyldene)-2-(2-fluoro-[1,1'-biphenyl]-4-yl)propanehydrazide (**20**). Color: Cream; Rf: 0.51 (*n*-hexane/ethyl acetate 25:75);  $^1H$ -NMR (400 MHz DMSO- $d_6$ )  $\delta$  1.45 (d,  $J = 6.8$  Hz, 3H), 3.42 (q,  $J = 6.8$  Hz, 1H), 7.23–7.25 (m, 5H), 7.36 (d,  $J = 7.4$  Hz, 2H), 7.58–7.60 (m, 3H), 8.25 (d,  $J = 7.4$  Hz, 2H), 8.48 (s, 1H), 11.68 (s, 1H); HRESI-MS  $[M + H]^+$  calcd for  $C_{22}H_{18}BrFN_2O$ , 424.0587, found, 425.2935.

*N'*-(2-Fluoro-4-methoxybenzylidene)-2-(2-fluoro-[1,1'-biphenyl]-4-yl)propanehydrazide (**21**). Color: Cream; Rf: 0.53 (*n*-hexane/ethyl acetate 25:75);  $^1H$ -NMR (400 MHz DMSO- $d_6$ )  $\delta$  1.39 (d,  $J = 7.3$  Hz, 3H), 3.47 (q,  $J = 7.3$  Hz, 1H), 3.91 (s, 3H), 7.25–7.27 (m, 5H), 7.42 (d,  $J = 7.4$  Hz, 1H), 7.49 (d,  $J = 7.4$  Hz, 2H), 7.51 (s, 1H), 7.59–7.61 (m, 2H), 8.40 (s, 1H), 11.58 (s, 1H); HRESI-MS  $[M + H]^+$  calcd for  $C_{23}H_{20}F_2N_2O_2$ , 394.1493, found, 394.4139.

*N'*-(4-Bromo-3,5-dimethoxybenzylidene)-2-(2-fluoro-[1,1'-biphenyl]-4-yl)propanehydrazide (**22**). Color: Cream; Rf: 0.52 (*n*-hexane/ethyl acetate 25:75);  $^1H$ -NMR (400 MHz DMSO- $d_6$ )  $\delta$  1.45 (d,  $J = 7.0$  Hz, 3H), 3.49 (q,  $J = 7.0$  Hz, 1H), 3.90 (s, 3H), 3.92 (s, 3H), 7.29–7.31 (m, 5H), 7.36 (s, 2H), 7.60–7.63 (m, 3H), 8.47 (s, 1H), 11.60 (s, 1H); HRESI-MS  $[M + H]^+$  calcd for  $C_{24}H_{22}BrFN_2O_3$ , 484.0798, found, 484.3455.

*N'*-(4-Bromo-2-fluorobenzyldene)-2-(2-fluoro-[1,1'-biphenyl]-4-yl)propanehydrazide (**23**). Color: Cream; Rf: 0.50

Table 1. *In Vitro* Urease Inhibitory Activity of Synthesized 2-[2-Fluoro[1,1'-biphenyl]-4-yl] Propanoic Acid Hydrazide Derivatives (4–31)<sup>a</sup>

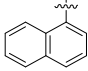
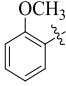
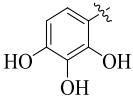
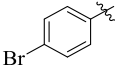
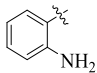
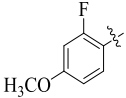
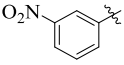
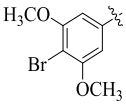
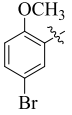
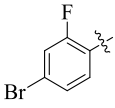
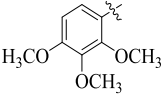
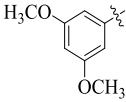
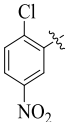
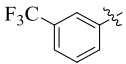
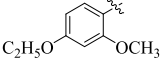
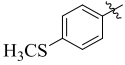
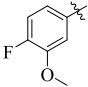
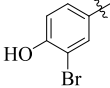
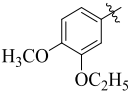
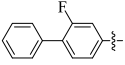
Compd	R	IC <sub>50</sub> ± SEM <sup>a</sup> (μM)	Compd	R	IC <sub>50</sub> ± SEM <sup>a</sup> (μM)
4		53.71 ± 3.81	19		55.74 ± 3.82
5		25.12 ± 1.13	20		58.77 ± 3.99
6		53.73 ± 3.82	21		89.75 ± 8.35
7		29.16 ± 1.12	22		90.75 ± 7.71
8		58.32 ± 3.34	23		86.85 ± 8.71
9		55.76 ± 3.04	24		79.23 ± 7.94
10		50.71 ± 5.17	25		59.54 ± 4.28
11		52.71 ± 3.56	26		78.01 ± 7.63
12		56.06 ± 4.89	27		80.00 ± 8.61
13		81.01 ± 8.43	28		58.53 ± 4.28

Table 1. continued

Compd	R	IC <sub>50</sub> ± SEM <sup>a</sup> (μM)	Compd	R	IC <sub>50</sub> ± SEM <sup>a</sup> (μM)
14		55.71 ± 3.71	29		57.51 ± 4.27
15		28.61 ± 1.73	30		18.92 ± 0.61
16		55.72 ± 3.82	31		28.12 ± 1.26
17		72.41 ± 3.61	<b>Thiourea (Standard) = 21.14 ± 0.425</b>		
18		26.46 ± 0.44			

<sup>a</sup>NA = not active; S.E.M. = standard error mean.

(*n*-hexane/ethyl acetate 25:75); <sup>1</sup>H-NMR (400 MHz DMSO-*d*<sub>6</sub>) δ 1.21 (d, *J* = 6.6 Hz, 3H), 3.49 (q, *J* = 6.6 Hz, 1H), 7.11–7.13 (m, 5H), 7.28 (d, *J* = 7.5 Hz, 1H), 7.60–7.63 (m, 3H), 7.36 (d, *J* = 1.5 Hz, 1H), 8.18 (d, *J* = 7.5 Hz, 1H), 8.54 (s, 1H), 11.57 (s, 1H); HRESI-MS [M + H]<sup>+</sup> calcd for C<sub>22</sub>H<sub>17</sub>BrF<sub>2</sub>N<sub>2</sub>O, 442.0492, found, 443.2840.

*N'*-(2,5-Dimethoxybenzylidene)-2-(2-fluoro-[1,1'-biphenyl]-4-yl)propanehydrazide (**24**). Color: Cream; *R*<sub>f</sub>: 0.52 (*n*-hexane/ethyl acetate 25:75); <sup>1</sup>H-NMR (400 MHz DMSO-*d*<sub>6</sub>) δ 1.22 (d, *J* = 6.7 Hz, 3H), 3.54 (q, *J* = 6.7 Hz, 1H), 3.76 (s, 3H), 3.90 (s, 3H), 6.90 (d, *J* = 7.0 Hz, 1H), 7.01–7.03 (m, 5H), 7.19 (s, 1H), 7.29 (d, *J* = 7.0 Hz, 1H), 7.46–7.48 (m, 3H), 8.51 (s, 1H), 11.49 (s, 1H); HRESI-MS [M + H]<sup>+</sup> calcd for C<sub>24</sub>H<sub>23</sub>FN<sub>2</sub>O<sub>3</sub>, 406.1693, found, 406.4494.

2-(2-Fluoro-[1,1'-biphenyl]-4-yl)-*N'*-(3-(trifluoromethyl)benzylidene)propanehydrazide (**25**). Color: Cream; *R*<sub>f</sub>: 0.50 (*n*-hexane/ethyl acetate 25:75); <sup>1</sup>H-NMR (400 MHz DMSO-*d*<sub>6</sub>) δ 1.43 (d, *J* = 6.9 Hz, 3H), 3.42 (q, *J* = 6.9 Hz, 1H), 7.43–7.45 (m, 5H), 7.59 (d, *J* = 7.5 Hz, 1H), 7.68–7.70 (m, 5H), 7.95 (d, *J* = 7.5 Hz, 1H), 8.57 (s, 1H), 11.48 (s, 1H); HRESI-MS [M + H]<sup>+</sup> calcd for C<sub>23</sub>H<sub>18</sub>F<sub>4</sub>N<sub>2</sub>O, 414.1355, found, 414.3953.

2-(2-Fluoro-[1,1'-biphenyl]-4-yl)-*N'*-(4-(methylthio)benzylidene)propanehydrazide (**26**). Color: Cream; *R*<sub>f</sub>: 0.52 (*n*-hexane/ethyl acetate 25:75); <sup>1</sup>H-NMR (400 MHz DMSO-*d*<sub>6</sub>) δ 1.41 (d, *J* = 7.1 Hz, 3H), 2.01 (s, 3H), 3.54 (q, *J* = 7.1 Hz, 1H), 7.25–7.27 (m, 5H), 7.29 (d, *J* = 7.8 Hz, 2H), 7.49–7.52 (m, 3H), 7.86 (d, *J* = 7.8 Hz, 2H), 8.47 (s, 1H), 11.57 (s, 1H); HRESI-MS [M + H]<sup>+</sup> calcd for C<sub>23</sub>H<sub>21</sub>FN<sub>2</sub>OS, 392.1358, found, 392.4891.

*N'*-(3-Bromo-4-hydroxybenzylidene)-2-(2-fluoro-[1,1'-biphenyl]-4-yl)propanehydrazide (**27**). Color: Cream; *R*<sub>f</sub>: 0.54 (*n*-hexane/ethyl acetate 25:75); <sup>1</sup>H-NMR (400 MHz DMSO-

*d*<sub>6</sub>) δ 1.33 (d, *J* = 6.8 Hz, 3H), 3.41 (q, *J* = 6.8 Hz, 1H), 7.23–7.26 (m, 5H), 7.29 (d, *J* = 7.0 Hz, 1H), 7.33 (d, *J* = 7.0 Hz, 1H), 7.89–7.91 (m, 3H), 8.21 (d, *J* = 1.2 Hz, 1H), 8.59 (s, 1H), 10.50 (br.s, 1H), 11.57 (s, 1H); HRESI-MS [M + H]<sup>+</sup> calcd for C<sub>22</sub>H<sub>18</sub>BrFN<sub>2</sub>O<sub>2</sub>, 440.0536, found, 441.2930.

2-(2-Fluoro-[1,1'-biphenyl]-4-yl)-*N'*-(2-fluoro-[1,1'-biphenyl]-4-yl)methylene)propanehydrazide (**28**). Color: Light brown; *R*<sub>f</sub>: 0.52 (*n*-hexane/ethyl acetate 25:75); <sup>1</sup>H-NMR (400 MHz DMSO-*d*<sub>6</sub>) δ 1.25 (d, *J* = 7.1 Hz, 3H), 3.42 (q, *J* = 7.1 Hz, 1H), 7.34–7.38 (m, 6H), 7.42 (s, 1H), 7.49 (d, *J* = 7.6 Hz, 2H), 7.55–7.61 (m, 5H), 7.83 (t, *J* = 7.0 Hz, 2H), 8.54 (s, 1H), 11.60 (s, 1H); HRESI-MS [M + H]<sup>+</sup> calcd for C<sub>28</sub>H<sub>22</sub>F<sub>2</sub>N<sub>2</sub>O, 440.1700, found, 440.4839.

2-(2-Fluoro-[1,1'-biphenyl]-4-yl)-*N'*-(5-methylthiophen-2-yl)methylene)propanehydrazide (**29**). Color: Light brown; *R*<sub>f</sub>: 0.52 (*n*-hexane/ethyl acetate 25:75); <sup>1</sup>H-NMR (400 MHz DMSO-*d*<sub>6</sub>) δ 1.20 (d, *J* = 7.0 Hz, 3H), 2.40 (s, 3H), 3.40 (q, *J* = 7.0 Hz, 1H), 6.89–6.92 (m, 6H), 7.12 (d, *J* = 7.6 Hz, 1H), 7.55–7.61 (m, 3H), 8.49 (s, 1H), 11.45 (s, 1H); HRESI-MS [M + H]<sup>+</sup> calcd for C<sub>21</sub>H<sub>19</sub>FN<sub>2</sub>OS, 366.1202, found, 366.4519.

*N'*-(2,3-Dihydroxybenzylidene)-2-(2-fluoro-[1,1'-biphenyl]-4-yl)propanehydrazide (**30**). Color: Cream; *R*<sub>f</sub>: 0.52 (*n*-hexane/ethyl acetate 25:75); <sup>1</sup>H-NMR (400 MHz DMSO-*d*<sub>6</sub>) δ 1.27 (d, *J* = 6.5 Hz, 3H), 3.43 (q, *J* = 6.5 Hz, 1H), 6.89 (d, *J* = 7.0 Hz, 1H), 7.17–7.19 (m, 5H), 7.26 (t, *J* = 7.0 Hz, 1H), 7.39 (d, *J* = 7.0 Hz, 1H), 7.82–7.85 (m, 3H), 8.46 (s, 1H), 10.50 (br.s, 2H), 11.55 (s, 1H); HRESI-MS [M + H]<sup>+</sup> calcd for C<sub>22</sub>H<sub>19</sub>FN<sub>2</sub>O<sub>3</sub>, 378.1379, found, 378.3964.

*N'*-(2-Nitrobenzylidene)-2-(2-fluoro-[1,1'-biphenyl]-4-yl)propanehydrazide (**31**). Color: Cream; *R*<sub>f</sub>: 0.50 (*n*-hexane/ethyl acetate 25:75); <sup>1</sup>H-NMR (400 MHz DMSO-*d*<sub>6</sub>) δ 1.32 (d, *J* = 6.6 Hz, 3H), 3.41 (q, *J* = 6.6 Hz, 1H), 7.26–7.29 (m, 5H), 7.37 (t, *J* = 8.5 Hz, 1H), 7.40 (d, *J* = 8.5 Hz, 1H), 7.84–

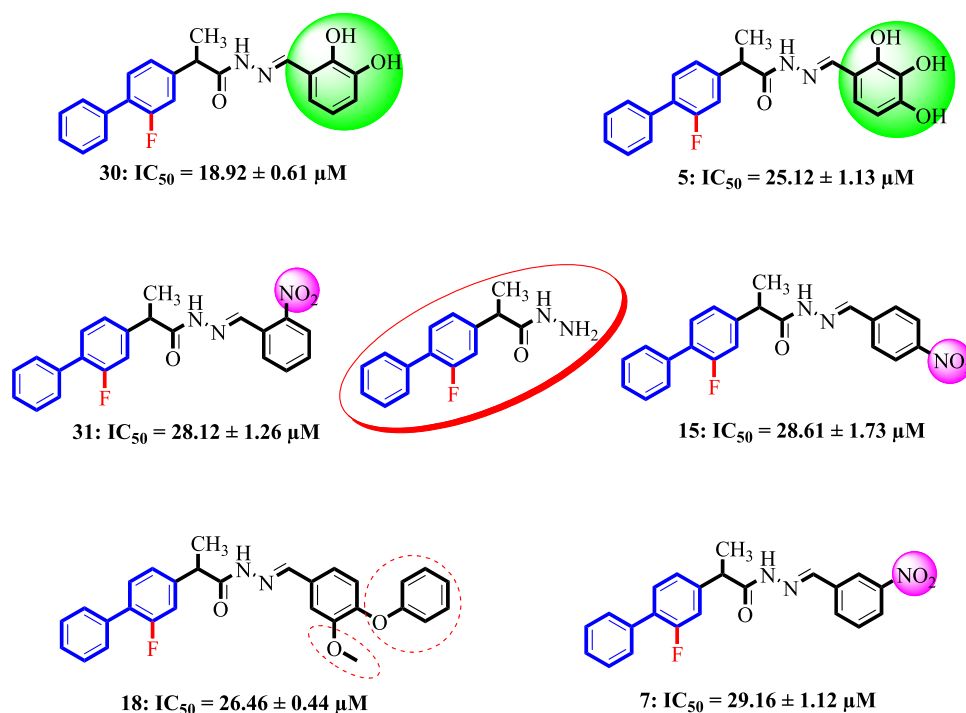


Figure 2. Most active compounds of the series.

7.87 (m, 3H), 7.89 (t,  $J = 8.5$  Hz, 1H), 8.26 (d,  $J = 8.5$  Hz, 1H), 8.59 (s, 1H), 11.74 (s, 1H); HRESI-MS  $[M + H]^+$  calcd for  $C_{22}H_{18}FN_3O_3$ , 391.1381, found, 391.4051.

## RESULTS AND DISCUSSION

**Chemistry.** Twenty-eight (28) different (*E*)-*N'*-benzylidene-2-(2-fluoro-[1,1'-biphenyl]-4-yl)propanehydrazide derivatives, 4–31, were synthesized by a two-step procedure.<sup>27,28</sup> In the first step, the commercially available 2-(2-fluoro-[1,1'-biphenyl]-4-yl)propanoic acid **1** was esterified in the presence of concentrated  $H_2SO_4$  and methanol by refluxing for 4–5 h. This was followed by the nucleophilic attack of hydrazine in the second step to give the corresponding hydrazides. In the third step, 2-(2-fluoro-[1,1'-biphenyl]-4-yl)propanehydrazide **3** was refluxed with different substituted aromatic aldehydes in the presence of the catalytic amount of glacial acetic acid in methanol to deliver (*E*)-*N'*-benzylidene-2-(2-fluoro-[1,1'-biphenyl]-4-yl)propanehydrazide derivatives 4–31 (Table 1).  $^1H$ -NMR and HR-ESI-MS were performed for the structure confirmation of the synthesized derivatives.

**In Vitro Urease Inhibitory Activity.** All of the synthesized compounds were screened for their *in vitro* urease inhibitory potential. All of the compounds showed urease inhibition in the range of  $IC_{50} = 18.92 \pm 0.61$  to  $90.75 \pm 7.71 \mu M$  as compared to the standard thiourea ( $IC_{50} = 21.14 \pm 0.425 \mu M$ ). The most active compound among the series was compound **30** with the  $IC_{50}$  value of  $18.92 \pm 0.61 \mu M$ , showing better activity than the standard thiourea. Similarly, compounds **5** ( $IC_{50} = 25.12 \pm 1.13 \mu M$ ), **18** ( $IC_{50} = 26.46 \pm 0.44 \mu M$ ), **31** ( $IC_{50} = 28.12 \pm 1.26 \mu M$ ), **15** ( $IC_{50} = 28.61 \pm 1.73 \mu M$ ), and **7** ( $IC_{50} = 29.16 \pm 1.12 \mu M$ ) showed potent activity close to those of the standard thiourea. However, compounds **10** ( $IC_{50} = 50.71 \pm 5.17 \mu M$ ), **11** ( $IC_{50} = 52.71 \pm 3.56 \mu M$ ), **4** ( $IC_{50} = 53.71 \pm 3.81 \mu M$ ), **6** ( $IC_{50} = 53.73 \pm 3.82 \mu M$ ), **14** ( $IC_{50} = 55.71 \pm 3.71 \mu M$ ), **16** ( $IC_{50} = 55.72 \pm 3.82 \mu M$ ), **19** ( $IC_{50} = 55.74 \pm 3.82 \mu M$ ), **9** ( $IC_{50} = 55.76 \pm 3.04$

$\mu M$ ), **12** ( $IC_{50} = 56.06 \pm 4.89 \mu M$ ), **29** ( $IC_{50} = 57.51 \pm 4.27 \mu M$ ), **8** ( $IC_{50} = 58.32 \pm 3.34 \mu M$ ), **28** ( $IC_{50} = 58.53 \pm 4.28 \mu M$ ), **20** ( $IC_{50} = 58.77 \pm 3.99 \mu M$ ), and **25** ( $IC_{50} = 59.54 \pm 4.28 \mu M$ ) have shown significant urease inhibitory activity. On the other hand, compounds **17** ( $IC_{50} = 72.41 \pm 3.61 \mu M$ ), **26** ( $IC_{50} = 78.01 \pm 7.63 \mu M$ ), **24** ( $IC_{50} = 79.23 \pm 7.94 \mu M$ ), **27** ( $IC_{50} = 80.00 \pm 8.61 \mu M$ ), **13** ( $IC_{50} = 81.01 \pm 8.43 \mu M$ ), **23** ( $IC_{50} = 86.85 \pm 8.71 \mu M$ ), **21** ( $IC_{50} = 89.75 \pm 8.35 \mu M$ ), and **22** ( $IC_{50} = 90.75 \pm 7.71 \mu M$ ) showed moderate activity compared with the standard thiourea (Table 1).

**Structure–Activity Relationship.** For better understanding, the structure–activity relationship of the synthesized analogues was analyzed by examining the alterations in location and nature of the attached substituent (R) on the benzene ring. Among the synthesized series, compound **30** was found to be the most active inhibitor of the urease enzyme with the  $IC_{50}$  value of  $18.92 \pm 0.61 \mu M$ , which was better than the standard thiourea. The excellent activity of compound **30** might be due to the presence of the electron-donating hydroxyl ( $-OH$ ) group attached at the 2- and 3-positions (*ortho*, *meta*) of the benzene ring (Figure 2). A comparison of compound **5** with compound **9** showed the higher activity of compound **5** with the  $IC_{50}$  value of  $25.12 \pm 1.13 \mu M$ , which could be due to the presence of three hydroxyl groups attached at the 2-, 3-, and 4-positions of the benzene ring, while the replacement of the hydroxyl substituent with the methoxy ( $-OCH_3$ ) substituent at the same position caused an insignificant change in the activity of compound **9** ( $IC_{50} = 55.76 \pm 3.04 \mu M$ ). However, a comparison of compound **31** ( $IC_{50} = 28.12 \pm 1.26 \mu M$ ), with **15** ( $IC_{50} = 28.61 \pm 1.73 \mu M$ ), **7** ( $IC_{50} = 29.16 \pm 1.12 \mu M$ ), and **6** ( $IC_{50} = 53.73 \pm 3.82 \mu M$ ) showed that a minor change occurred in the activity of compounds **31** and **6** because of the change in the position of the same nitro substituent attached at the *ortho* and *para* positions of the benzene ring. Likewise, the decrease in the activity of compound **6** can be due to the existence of the amine

Table 2. Docking Scores (S) and Interaction Details of the Selected Active Compounds

no	docking score	ligand	receptor	interaction details		
				interaction	distance (Å°)	E (kcal/mol)
4	-6.0780	N 12 O	CYS 322 (C)	H-donor	3.03	-2.3
5	-7.1888	O 8 O	LEU 365 (C)	H-donor	2.98	-0.5
		C 20 ND1	HIS 323 (C)	H-donor	3.20	-0.6
6	-6.8182	6-ring CB	MET 367 (C)	pi-H	3.73	-0.3
		N 7 OD2	ASP 363 (C)	H-donor	3.41	-0.8
		N 10 CA	ALA 170 (C)	H-acceptor	3.03	-1.3
7	-10.002	O 7 O	ALA 170 (C)	H-donor	3.05	0.4
		O 8 O	GLY 280 (C)	H-donor	2.71	-2.5
8	-9.0570	N 11 CA	ALA 170 (C)	H-acceptor	3.14	-1.3
		N 9 O	CYS 322 (C)	H-donor	2.63	-3.9
9	-7.5075	6-ring CA	CYS 322 (C)	pi-H	4.00	-0.8
		C 32 OX2	KCX 220 (C)	H-donor	2.82	-1.4
10	-6.5217	C 32 OD2	ASP 363 (C)	H-donor	2.59	-1.0
		N 9 O	CYS 322 (C)	H-donor	3.16	-1.7
12	-8.5273	N 8 O	CYS 322 (C)	H-donor	2.74	-3.4
13	-6.3806	6-ring 5-ring	HIS 324 (C)	pi-pi	3.53	-0.2
14	-7.2759	C 28 OX2	KCX 220 (C)	H-donor	3.16	-1.2
		O 10 CA	HIS 323 (C)	H-acceptor	2.79	-1.2
15	-4.2119	O 29 SD	MET 367 (C)	H-donor	3.57	-0.6
16	-4.1236	N 9 OD2	ASP 224 (C)	H-donor	2.32	45.7
18	-4.0724	6-ring 5-ring	HIS 323 (C)	pi-pi	3.48	-0.0
19	-8.4998	O 10 CB	ALA 170 (C)	H-acceptor	3.06	-0.8
		O 27 NE2	HIS 222 (C)	H-acceptor	2.47	-2.3
20	-7.7970	S 5 O	LYS 169 (C)	H-donor	4.11	-1.2
		S 5 OD2	ASP 363 (C)	H-donor	4.09	-1.1
		5-ring NE2	HIS 222 (C)	pi-H	4.20	-3.1
		5-ring CB	MET 367 (C)	pi-H	4.33	-0.6
25	-5.7119	C 11 OE2	GLU 166 (C)	H-donor	2.86	-1.4
		C 17 O	ALA 170 (C)	H-donor	2.65	-0.2
26	-5.0962	6-ring 5-ring	HIS 323 (C)	pi-pi	3.72	-0.1
		N 8 O	CYS 322 (C)	H-donor	2.99	-2.7
28	-5.6220	S 27 SD	MET 318 (C)	H-donor	4.49	-0.3
		N 16 CE	LYS 169 (C)	H-acceptor	3.37	-0.6
29	-6.1851	BR 7 NE2	HIS 137 (C)	H-donor	3.09	-2.9
		6-ring NE2	HIS 222 (C)	pi-H	3.70	-0.8
		6-ring CA	ALA 366 (C)	pi-H	4.76	-0.6
30	-8.394	C 6 O	ALA 170 (C)	H-donor	2.99	-1.6
		6-ring NH <sub>2</sub>	ARG 339 (C)	pi-cation	4.15	-1.4
31	-7.7046	6-ring NH <sub>2</sub>	ARG 339 (C)	pi-cation	3.64	-0.7
		O 28 NI	NI 799 (C)	metal	2.44	-1.4
		O 29 NI	NI 798 (C)	metal	2.31	-1.2

(-NH<sub>2</sub>) group attached at the *ortho* position of the benzene ring, while the higher activity of compounds 31, 15, and 6 may be due to the presence of the electron-withdrawing nitro (-NO<sub>2</sub>) group attached at the *ortho*, *para*, and *meta* positions of the benzene ring, respectively. The decrease that occurs in the activity of compound 17 (IC<sub>50</sub> = 72.41 ± 3.61 μM) might be due to the presence of the phenoxy group attached at the *para* position of the benzene ring, while the increase in the urease inhibitory activity of compound 18 (IC<sub>50</sub> = 26.46 ± 0.44 μM) is due to the attachment of the methoxy group at the *meta* position and the phenoxy group at the *para* position of the benzene ring (Table 1).

**Molecular Docking and Interactions Report.** For predicting the mechanism of inhibition of the synthesized derivatives, indicated by the kinetic study, molecular docking of the active compounds was performed using the crystalline structure of the urease enzyme. The most satisfactory docking

conformations of all active compounds were detected inside the active sites with proper alignment. Both the hydrophilic and hydrophobic amino acids were part of the active site.

Arg 339, Asp 224, 363, Asp 494 Glu 166, 223, and His 323, 324 are examples of hydrophilic amino acids, while hydrophobic amino acids included Ala 170, 366, Cys 322, Lys 169, Leu 319, and Met 637. The key amino acids and ligands were linked by two Ni ions of urease. Interactions of nearly all conformations of all ligands were observed with significant residues inside the pocket. The GBVI/WSA binding free energy scores were calculated and the data was used for ranking the docked poses. Additionally, the most capable docked conformation of every compound was assessed for binding mode. Docking results details are given in Table 2. Polar bonds, hydrogen bonding, π-π and π-H interactions played key roles in the binding mode of the active compounds with active site residues and a healthy assignment with the



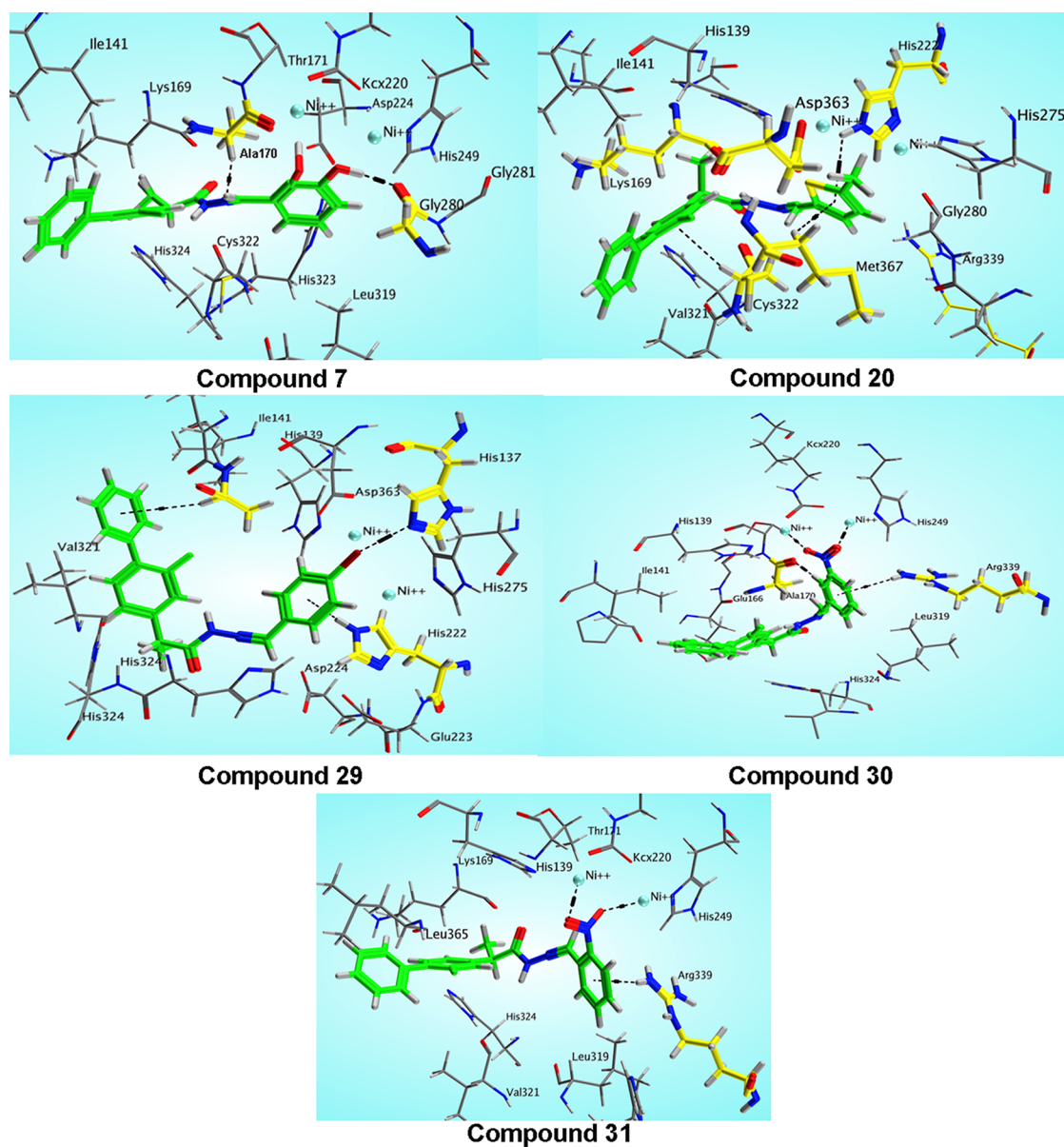


**Figure 3.** Three-dimensional (3D) interactions of compounds 7, 20, 29, 30, and 31 with active site residues of urease. Ligands are shown as green sticks. Key residues of the active site are shown as yellow sticks. Hydrogen bonding and other interaction are shown as dark-colored dotted lines.

backbone of the enzyme was observed. 3-D interactions of some promising inhibitors are presented (Figure 3).

## CONCLUSIONS

Twenty-eight new substituted acyl hydrazones of (*E*)-*N'*-benzylidene-2-(2-fluoro-[1,1'-biphenyl]-4-yl)propanehydrazide (4–31) were synthesized by the condensation of aromatic aldehydes and the commercially available 2-(2-fluoro-[1,1'-biphenyl]-4-yl) propanoic acid in good to excellent yields. All of the synthesized derivatives were characterized *via* different spectroscopic techniques such as HREI-MS and <sup>1</sup>H-NMR and finally evaluated for *in vitro* urease inhibitory activity. All of the synthesized analogues demonstrated good inhibitory activities in the range of  $IC_{50} = 18.92 \pm 0.61$  to  $90.75 \pm 7.71 \mu\text{M}$  compared with the standard thiourea ( $IC_{50} = 21.14 \pm 0.42 \mu\text{M}$ ). Compound 30 was found to be the most active among the series better than the standard thiourea. SAR revealed that the electron-donating groups in the phenyl ring have more

influence on enzyme inhibition. However, to gain insight into the participation of different substituents in the synthesized derivatives on the binding interactions with urease enzyme, *in silico* molecular modeling analysis was carried out.

## ASSOCIATED CONTENT

### Supporting Information

The Supporting Information is available free of charge at <https://pubs.acs.org/doi/10.1021/acsomega.2c05498>.

Scheme S1 and Table S1 show the synthesized compounds, Table S2 shows the docking scores (*S*) and interaction details of the selected active compounds; Figure S1 shows the justification of the current study, Figure S2 shows the most active compounds of the series, Figure S3 shows the three-dimensional (3D) interactions of compounds, Figures S4–S12 show <sup>1</sup>H NMR and mass spectra of the prepared compounds 4, 7, 19, 20, and 22 (PDF)

## AUTHOR INFORMATION

## Corresponding Author

Momin Khan – Department of Chemistry, Abdul Wali Khan University, Mardan 23200, Pakistan; [orcid.org/0000-0003-0936-5025](https://orcid.org/0000-0003-0936-5025); Phone: +92937929122; Email: [mominkhan@awkum.edu.pk](mailto:mominkhan@awkum.edu.pk)

## Authors

Sajjad Ahmad – Department of Chemistry, Abdul Wali Khan University, Mardan 23200, Pakistan

Muhammad Ishaq Ali Shah – Department of Chemistry, Abdul Wali Khan University, Mardan 23200, Pakistan

Mahboob Ali – Department of Chemistry, Government Degree college, Mardan 23200, Pakistan

Aftab Alam – Department of Chemistry, University of Malakand, Chakdara 18800, Pakistan

Muhammad Riaz – Department of Chemistry, Government Degree college Garhi Kapura, Mardan 23200, Pakistan

Khalid Mohammed Khan – H. E. J. Research Institute of Chemistry, International Center for Chemical and Biological Sciences, University of Karachi, Karachi 75270, Pakistan; [orcid.org/0000-0001-8337-4021](https://orcid.org/0000-0001-8337-4021)

Complete contact information is available at:

<https://pubs.acs.org/10.1021/acsomega.2c05498>

## Notes

The authors declare no competing financial interest.

## ACKNOWLEDGMENTS

The authors are highly thankful to the University of Nizwa, Oman, for providing the facility of Molecular Operating Environment (MOE) software.

## REFERENCES

- (1) Ahmed, M.; Qadir, M. A.; Hameed, A.; Arshad, M. N.; Asiri, A. M.; Muddassar, M. Azomethines, isoxazole, *N*-substituted pyrazoles and pyrimidine containing curcumin derivatives: Urease inhibition and molecular modeling studies. *Biochem. Biophys. Res. Commun.* **2017**, *490*, 434–440.
- (2) Peek, R. M.; Blaser, M. J. *Helicobacter pylori* and gastrointestinal tract adenocarcinomas. *Nat. Rev. Cancer* **2002**, *2*, 28–37.
- (3) Sudkolai, S. T.; Nourbakhsh, F. Urease activity as an index for assessing the maturity of cow manure and wheat residue vermicomposts. *Waste Manage.* **2017**, *64*, 63–66.
- (4) Taha, M.; Shah, S. A. A.; Khan, A.; Arshad, F.; Ismail, N. H.; Afifi, M.; Imran, S.; Choudhary, M. I. Synthesis of 3, 4, 5-trihydroxybenzohydrazone and evaluation of their urease inhibition potential. *Arabian J. Chem.* **2019**, *12*, 2973–2982.
- (5) Upadhyay, V.; Poroyko, V.; Kim, T.-j.; Devkota, S.; Fu, S.; Liu, D.; Tumanov, A. V.; Koroleva, E. P.; Deng, L.; Nagler, C.; et al. Lymphotoxin regulates commensal responses to enable diet-induced obesity. *Nat. Immunol.* **2012**, *13*, 947–953.
- (6) Shamim, S.; Khan, K. M.; Salar, U.; Ali, F.; Lodhi, M. A.; Taha, M.; Khan, F. A.; Ashraf, S.; Ul-Haq, Z.; Ali, M.; Perveen, S. 5-Acetyl-6-methyl-4-aryl-3, 4-dihydropyrimidin-2 (1H)-ones: As potent urease inhibitors; synthesis, in vitro screening, and molecular modeling study. *Bioorg. Chem.* **2018**, *76*, 37–52.
- (7) Khan, M.; Alam, A.; Khan, K. M.; Salar, U.; Chigurupati, S.; Wadood, A.; Ali, F.; Mohammad, J. I.; Riaz, M.; Perveen, S. Flurbiprofen derivatives as novel  $\alpha$ -amylase inhibitors: Biology-oriented drug synthesis (BIODS), in vitro, and in silico evaluation. *Bioorg. Chem.* **2018**, *81*, 157–167.
- (8) Mohammed Khan, K.; Rahim, F.; Ambreen, N.; Taha, M.; Khan, M.; Jahan, H.; Shaikh, A.; Iqbal, S.; Perveen, S.; Iqbal Choudhary, M. Synthesis of benzophenonehydrazone Schiff bases and their in vitro antiglycating activities. *Med. Chem.* **2013**, *9*, 588–595.
- (9) Pedrood, K.; Azizian, H.; Montazer, M. N.; Mohammadi-Khanaposhtani, M.; Mohammadi-Khanaposhtani, M.; Asgari, M. S.; Asadi, M.; Bahadorikhalili, S.; Rastegar, H.; Larijani, B.; Amanlou, M. Arylmethylene hydrazine derivatives containing 1, 3-dimethylbarbituric moiety as novel urease inhibitors. *Sci. Rep.* **2021**, *11*, No. 10607.
- (10) Fan, Y.; He, Y.; Liu, X.; Hu, T.; Ma, H.; Yang, X.; Luo, X.; Huang, G. Iodine-mediated domino oxidative cyclization: one-pot synthesis of 1, 3, 4-oxadiazoles via oxidative cleavage of C (sp<sup>2</sup>)–H or C (sp)–H bond. *J. Org. Chem.* **2016**, *81*, 6820–6825.
- (11) Shamim, S.; Khan, K. M.; Ullah, N.; Mahdavi, M.; Faramarzi, M. A.; Larijani, B.; Salar, U.; Rafique, R.; Taha, M.; Perveen, S. Synthesis, In Vitro, and In Silico Evaluation of Indazole Schiff Bases as Potential  $\alpha$ -Glucosidase Inhibitors. *J. Mol. Struct.* **2021**, No. 130826.
- (12) Jamil, W.; Perveen, S.; Shah, S. A. A.; Taha, M.; Ismail, N. H.; Perveen, S.; Ambreen, N.; Khan, K. M.; Choudhary, M. I. Phenoxyacetohydrazide Schiff bases:  $\beta$ -Glucuronidase inhibitors. *Molecules* **2014**, *19*, 8788–8802.
- (13) Mohamad, S.; Yunus, W. M. Z. W.; Haron, M. J.; Rahman, M. Z. A. Enzymatic synthesis of fatty hydrazides from palm oils. *J. Oleo Sci.* **2008**, *57*, 263–267.
- (14) Khan, M.; Ahad, G.; Manaf, A.; Naz, R.; Hussain, S. R.; Deeba, F.; Shah, S.; Khan, A.; Ali, M.; Zaman, K.; et al. Synthesis, in vitro urease inhibitory activity, and molecular docking studies of (perfluorophenyl) hydrazone derivatives. *Med. Chem. Res.* **2019**, *28*, 873–883.
- (15) Nilsson, J.; Rüetschi, U.; Halim, A.; Hesse, C.; Carlsohn, E.; Brinkmalm, G.; Larson, G. Enrichment of glycopeptides for glycan structure and attachment site identification. *Nat. Methods* **2009**, *6*, 809–811.
- (16) Ahad, G.; Khan, M.; Khan, A.; Ibrahim, M.; Salar, U.; Khan, K. M.; Perveen, S. Synthesis, structural characterization, and antioxidant activities of 2, 4-dinitrophenyl-hydrazone derivatives. *J. Chem. Soc. Pak.* **2018**, *40*, 961.
- (17) Zhang, H.; Li, X.-j.; Martin, D. B.; Aebersold, R. Identification and quantification of N-linked glycoproteins using hydrazone chemistry, stable isotope labeling and mass spectrometry. *Nat. Biotechnol.* **2003**, *21*, 660–666.
- (18) Wayua, C.; Roy, J.; Putt, K. S.; Low, P. S. Selective tumor targeting of desacetyl vinblastine hydrazide and tubulysin B via conjugation to a cholecystokinin 2 receptor (CCK2R) ligand. *Mol. Pharmaceutics* **2015**, *12*, 2477–2483.
- (19) Priegue, J. M.; Lostalé-Seijo, I.; Crisan, D.; Granja, J. R.; Fernández-Trillo, F.; Montenegro, J. Different-length hydrazone activated polymers for plasmid DNA condensation and cellular transfection. *Biomacromolecules* **2018**, *19*, 2638–2649.
- (20) Rubin, B.; Antonaccio, M.; Horovitz, Z. The Renin-Angiotensin System, Converting Enzyme Inhibition, and Antihypertensive Therapy. *Prog. Horm. Biochem. Pharmacol.* **1980**, *1*–53.
- (21) Gomez, H. J.; Cirillo, V. J.; Davies, R. O.; Bolognese, J. A.; Walker, J. F. Enalapril in congestive heart failure: acute and chronic invasive hemodynamic evaluation. *Int. J. Cardiol.* **1986**, *11*, 37–48.
- (22) Bhattacharjee, I.; Mazumdar, D.; Saha, S. P. Microbial amylases and their potential application in industries: A review. *The Pharma Innovation Journal* **2019**, *8*, 162–170.
- (23) Naheed, N.; Maher, S.; Saleem, F.; Khan, A.; Wadood, A.; Rasheed, S.; Choudhary, M. I.; Froeyen, M.; Abdullah, I.; Mirza, M. U.; et al. New isolate from *Salvinia molesta* with antioxidant and urease inhibitory activity. *Drug Dev. Res.* **2021**, *82*, 1169–1181.
- (24) Achar, K. C.; Hosamani, K. M.; Seetharamareddy, H. R. In-vivo analgesic and anti-inflammatory activities of newly synthesized benzimidazole derivatives. *Eur. J. Med. Chem.* **2010**, *45*, 2048–2054.
- (25) Amdekar, S.; Roy, P.; Singh, V.; Kumar, A.; Singh, R.; Sharma, P. Anti-inflammatory activity of lactobacillus on carrageenan-induced paw edema in male wistar rats. *Int. J. Inflammation* **2012**, *2012*, No. 752015.

- (26) Bacchi, S.; Palumbo, P.; Sponta, A.; Coppolino, M. F. Clinical pharmacology of non-steroidal anti-inflammatory drugs: a review. *Anti-Inflammatory Anti-Allergy Agents Med. Chem.* **2012**, *11*, 52–64.
- (27) Chappell, A. G.; Bai, J.; Yuksel, S.; Ellis, M. F. Post-mastectomy pain syndrome: defining perioperative etiologies to guide new methods of prevention for plastic surgeons. *World J Plast Surg.* **2020**, *9*, 247–253.
- (28) Cipriano, M.; Björklund, E.; Wilson, A. A.; Congiu, C.; Onnis, V.; Fowler, C. J. Inhibition of fatty acid amide hydrolase and cyclooxygenase by the N-(3-methylpyridin-2-yl) amide derivatives of flurbiprofen and naproxen. *Eur. J. Pharmacol.* **2013**, *720*, 383–390.
- (29) Davis, A.; Robson, J. The dangers of NSAIDs: look both ways. *Brit. J. Gener Pract.* **2016**, *66*, 172–173.
- (30) Domiati, S.; El-Mallah, A.; Ghoneim, A.; Bekhit, A.; El Razik, H. A. Evaluation of anti-inflammatory, analgesic activities, and side effects of some pyrazole derivatives. *Inflammopharmacology* **2016**, *24*, 163–172.
- (31) Abbas, S.; Zaib, S.; Ali, S.; Iqbal, J. 15-LOX Inhibitors: Biochemical Evaluation of Flurbiprofen and its Derivatives. *Life and Science* **2020**, *1*, 92–97.
- (32) Eriksen, J. L.; Sagi, S. A.; Smith, T. E.; Weggen, S.; Das, P.; McLendon, D.; Ozols, V. V.; Jessing, K. W.; Zavitz, K. H.; Koo, E. H.; Golde, T. E. NSAIDs and enantiomers of flurbiprofen target  $\gamma$ -secretase and lower A $\beta$ 42 in vivo. *J. Clin. Invest.* **2003**, *112*, 440–449.
- (33) Gasparini, L.; Ongini, E.; Wilcock, D.; Morgan, D. Activity of flurbiprofen and chemically related anti-inflammatory drugs in models of Alzheimer's disease. *Brain Res. Rev.* **2005**, *48*, 400–408.
- (34) Geerts, H. Drug evaluation: (R)-flurbiprofen—an enantiomer of flurbiprofen for the treatment of Alzheimer's disease. *IDrugs* **2007**, *10*, 121–133.
- (35) Tian, C.; Qiang, X.; Song, Q.; Cao, Z.; Ye, C.; He, Y.; Deng, Y.; Zhang, L. Flurbiprofen-chalcone hybrid Mannich base derivatives as balanced multifunctional agents against Alzheimer's disease: Design, synthesis and biological evaluation. *Bioorg. Chem.* **2020**, *94*, No. 103477.
- (36) Sozio, P.; Marinelli, L.; Cacciatore, I.; Fontana, A.; Türkez, H.; Giorgioni, G.; Ambrosini, D.; Barbato, F.; Grumetto, L.; Pacella, S.; et al. New flurbiprofen derivatives: Synthesis, membrane affinity and evaluation of in vitro effect on  $\beta$ -amyloid levels. *Molecules* **2013**, *18*, 10747–10767.
- (37) Taha, M.; Naz, H.; Rasheed, S.; Ismail, N. H.; Rahman, A. A.; Yousuf, S.; Choudhary, M. I. Synthesis of 4-methoxybenzoylhydrazones and evaluation of their antiglycation activity. *Molecules* **2014**, *19*, 1286–1301.
- (38) Taha, M.; Ismail, N. H.; Imran, S.; Wadood, A.; Rahim, F.; Saad, S. M.; Khan, K. M.; Nasir, A. Synthesis, molecular docking and  $\alpha$ -glucosidase inhibition of 5-aryl-2-(6'-nitrobenzofuran-2'-yl)-1, 3, 4-oxadiazoles. *Bioorg. Chem.* **2016**, *66*, 117–123.
- (39) Bushra; Shamim, S.; Khan, K. M.; Ullah, N.; Mahdavi, M.; Faramarzi, M. A.; Larijani, B.; Salar, U.; Rafique, R.; Taha, M.; Perveen, S. Synthesis, in vitro, and in silico evaluation of Indazole Schiff bases as potential  $\alpha$ -glucosidase inhibitors. *J. Mol. Struct.* **2021**, *1242*, 130826.
- (40) Ikram, M.; Khan, M.; Ahmad, S.; Rehman, S.; Schulzke, C. The crystal structure of 4-tert-butyl-N'-[(E)-(4-fluoro-3-methoxyphenyl)methylidene] benzohydrazide, C<sub>19</sub>H<sub>21</sub>F N<sub>2</sub>O<sub>2</sub>. *Z. Kristallogr. - New Cryst. Struct.* **2018**, *233*, 643–645.
- (41) Mao, W.-J.; Lv, P.-C.; Shi, L.; Li, H.-Q.; Zhu, H.-L. Synthesis, molecular docking and biological evaluation of metronidazole derivatives as potent *Helicobacter pylori* urease inhibitors. *Bioorg. Med. Chem.* **2009**, *17*, 7531–7536.
- (42) Alam, A.; Ali, M.; Rehman, N. U.; Ullah, S.; Halim, S. A.; Latif, A.; Khan, A.; Ullah, O.; Ahmad, S.; Al-Harrasi, A.; et al. Bio-Oriented Synthesis of Novel (S)-Flurbiprofen Clubbed Hydrazone Schiff's Bases for Diabetic Management: In Vitro and In Silico Studies. *Pharmaceuticals* **2022**, *15*, 672.
- (43) Akyüz, G. Synthesis and urease inhibition studies of some new quinazolinones. *J. Heterocycl. Chem.* **2021**, *58*, 1164–1170.
- (44) Patel, R.; Singh, B.; Sharma, A.; Saraswat, J.; Dohare, N.; ud din Parray, M.; Khan, A. A.; et al. Interaction and esterase activity of albumin serums with orphenadrine: A spectroscopic and computational approach. *J. Mol. Struct.* **2021**, *1239*, No. 130522.